

Effect of ZnO incorporation on Cu–Ni/Al₂O₃ catalyst for glycerol hydrogenolysis in the absence of added hydrogen

Tao Jiang¹ · Danni Kong¹ · Kun Xu³ · Fahai Cao^{1,2}

Received: 11 June 2015 / Accepted: 3 July 2015 / Published online: 23 July 2015
© The Author(s) 2015. This article is published with open access at Springerlink.com

Abstract A series of Cu–Ni bimetallic catalysts were developed and used for glycerol hydrogenolysis to produce 1,2-propanediol in the absence of added hydrogen along with the isopropanol as hydrogen donor. The monometallic Cu catalyst can catalyze the dehydrogenation of isopropanol effectively, but the Cu species would be oxidized to Cu⁺ which led to the catalyst deactivation. Ni incorporation can change the reduction behavior of Cu catalyst and the formation of Cu–Ni alloy might promote the hydrogenation of acetol. Furthermore, the effect of ZnO incorporation on the catalytic performance of Cu–Ni/Al₂O₃ bimetallic catalyst for glycerol hydrogenolysis in the absence of added hydrogen was investigated. The addition of ZnO enhanced the acidity of catalyst surface, resulting in higher C–O bond cleavage activity. Comparing the H₂-TPR profiles of Cu–Ni/Al₂O₃ with Cu–Ni/ZnO–Al₂O₃, it could be clearly observed that the reduction temperature was decreased remarkably by the addition of ZnO. XRD and SEM images revealed that the addition of ZnO inhibited the catalyst sintering and favored the formation of the strong interaction between Cu–Ni species and Al₂O₃ by the formation of the ZnAl₂O₄ phase.

Keywords Glycerol · 1,2-propanediol · Catalytic transfer hydrogenation · Bimetallic catalyst

Introduction

The excessive exploitation of fossil oil and gas brings about the energy depletion and environmental pollution, which greatly restrict human existence and economic development [1, 2]. In this context, biomass-derived resources are considered as renewable alternatives to obtain fuels and chemicals [3, 4]. In recent years, the rapid development of biodiesel production enriched the yield of glycerol and consequently reduced its market price. Wide investigations have been performed to convert glycerol to fuels and value-added chemicals. It is a resource-utilization efficient and biological technical process to employ glycerol hydrogenolysis for glycols (1,2-propanediol, ethylene glycol and 1,3-propanediol) generation [5, 6]. In published works, great valuable progresses have been made using noble metal catalysts (Pt, Ru, Rh, Pd, etc.) [7–10] as well as non-noble metal catalysts (Cu, Ni, Co, etc.) [11–13]. However, all the reported processes were carried out with external added hydrogen, which had several drawbacks: (1) hydrogenolysis reaction must be performed at high hydrogen pressure and high temperature owing to the low solubility of hydrogen in aqueous or organic glycerol solutions; (2) molecular hydrogen was produced in energy-intensive processes from fossil resources that raised the cost of equipment and transportation.

If the required hydrogen could be “in situ” generated in the active sites of the catalyst, the above problems caused by hydrogen accessibility would be solved. There were two different processes developed by researchers: aqueous phase reforming (APR) [14, 15] and catalytic transfer

✉ Fahai Cao
fhcao@ecust.edu.cn

¹ Engineering Research Center of Large Scale Reactor Engineering and Technology, Ministry of Education, East China University of Science and Technology, No. 130, Meilong Road, Shanghai 200237, China

² Key Laboratory of Chemical Engineering, East China University of Science and Technology, No. 130, Meilong Road, Shanghai 200237, China

³ East China Chemical Engineering Inc., No. 130, Meilong Road, Shanghai 200237, China

hydrogenation (CTH) [16, 17]. Of the two processes, CTH, in which hydrogen was transferred from a hydrogen donor molecule to an acceptor, avoided the carbon consuming via the reforming step and possessed more advantages and better application prospect. Musolino et al. [18] prepared a 10Pd/Fe₂O₃ catalyst by coprecipitation and used for selective conversion of glycerol to 1,2-propanediol (1,2-PDO) via CTH along with ethanol and isopropanol (2-PO) as hydrogen donor. Under the conditions of 180 °C and 0.5 MPa of inert atmosphere, glycerol conversion and 1,2-PDO selectivity reached 100 and 94 %, respectively. Gandarias [19] also found that CTH with formic acid was more efficient for the production of 1,2-PDO than in glycerol APR over Ni–Cu bimetallic catalyst under nitrogen pressure. Combined with a mechanistic study, they believed that hydrogen species come from dehydrogenation of formic acid and glycerol was converted to 1,2-PDO directly through intermediate alkoxide formation. Xia et al. [20] also prepared a Cu_{0.4}/Mg_{6.28}Al_{1.32}O_{8.26} catalyst by coprecipitation used for hydrogen-free synthesis of 1,2-PDO. They found that the enhanced basicity of catalysts and Cu active sites were the keys of the excellent catalytic performance.

In this work, a series of Cu–Ni/Al₂O₃ bimetallic catalysts were prepared by coprecipitation to selectively convert glycerol into 1,2-PDO in the absence of externally added hydrogen. The influence of Cu/Ni mass ratio on the catalytic performance was investigated and the synergistic effect between the two kinds of metals was studied by catalyst characterization. We also explored the promotion effect of ZnO introduction on the structure, reduction, catalyst stability and catalytic performance. In the end, the reaction pathways were also discussed.

Experimental

Catalyst preparation

All catalysts were prepared by the coprecipitation method. Typical synthesis for 1 g of 15Cu–15Ni/Al₂O₃ catalyst was carried out as follows: 0.5703 g of Cu(NO₃)₂·3H₂O, 0.7433 g Ni(NO₃)₂·6H₂O and 7.3584 g Al(NO₃)₃·9H₂O were dissolved into a 250 ml deionized water at room temperature under stirring. Then, 1.0 mol/l Na₂CO₃ solution was added dropwise to the mixed solution until the pH of the final solution reached 8.5 ± 0.1. After stirring and aging for overnight at room temperature, the obtained precipitate was filtrated, washed with 250 ml deionized water each for ten times, air-dried at 110 °C overnight, gently grounded by pestle and mortar and sieved to get the particles in the range of 40–60 mesh. Then, the catalyst was calcined in air at 550 °C for 4 h. Before use, the sample

was reduced in a flowing stream of hydrogen at a steady rate of 50 ml/min in a tube furnace at 500 °C for 4 h.

Catalysts of 30 wt % Cu/Al₂O₃, 25 wt % Cu–5 wt % Ni/Al₂O₃, 20 wt % Cu–10 wt % Ni/Al₂O₃, 15 wt % Cu–15 wt % Ni/Al₂O₃, 10 wt % Cu–20 wt % Ni/Al₂O₃, 5 wt % Cu–25 wt % Ni/Al₂O₃, 30 wt % Ni/Al₂O₃ were marked as 30Cu/Al₂O₃, 25Cu–5Ni/Al₂O₃, 20Cu–10Ni/Al₂O₃, 15Cu–15Ni/Al₂O₃, 10Cu–20Ni/Al₂O₃, 5Cu–25Ni/Al₂O₃, 30Ni/Al₂O₃, respectively. In a similar procedure, ZnO-promoted 15Cu–15Ni/Al₂O₃ catalysts were prepared by adding desired amount of Zn(NO₃)₂·6H₂O into the aqueous solution containing nickel, cobalt and aluminum before coprecipitation. 20, 40, 60, 80 and 100 wt % of ZnO addition to 15Cu–15Ni/Al₂O₃ were denoted as 15Cu–15Ni/20ZnO–Al₂O₃, 15Cu–15Ni/40ZnO–Al₂O₃, 15Cu–15Ni/60ZnO–Al₂O₃, 15Cu–15Ni/80ZnO–Al₂O₃, 15Cu–15Ni/100ZnO–Al₂O₃, respectively.

Catalyst characterization

N₂ adsorption–desorption isotherms of the prepared catalysts were obtained with a Micromeritics ASAP 2020 M instrument at liquid nitrogen temperature. Prior to N₂ adsorption, all samples were degassed at 200 °C for 6 h.

The X-ray diffraction patterns of the prepared catalysts were carried out on a Rigaku D/max-2550 diffractometer using Ni-filtered CuK_α radiation ($\lambda = 0.15406$ nm) at room temperature. The X-ray tube was operated at 40 kV, 100 mA and scanned from 10° to 80°. Identification of the crystalline phases was determined by checking JCPDS cards.

H₂-TPR of the catalysts was carried out on a Micromeritics AutoChem II 2920 instrument. Before the TPR experiments, catalysts were pretreated in argon stream at 300 °C for 60 min and then cooled to room temperature. The measurements were performed in a flow of 10 % volume fraction of H₂ in Ar mixture gas at a flow rate of 50 ml/min with a temperature ramp of 10 °C/min. H₂ consumption was continuously monitored by a thermal conductivity detector.

SEM images were taken on a Nova NanoSEM 450 instrument. Samples were coated with platinum using sputter coating to avoid charging. Analysis was carried out at an accelerating voltage of 15 kV.

Activity testing

Glycerol hydrogenolysis reactions were performed in a 250 ml stainless steel autoclave equipped with a stirrer, an electric temperature controller and a sample port for liquid samples. Prior to the reaction, 100 ml of 10 wt% glycerol isopropanol solution and 1.0 g reduced catalysts were loaded into the reactor and the autoclave was purged with

nitrogen to remove air for five times. Then, the autoclave was pressurized with N_2 to 1.0 MPa and heated to the required temperature. The rotation rate of the stirrer was set constant at 500 rpm throughout the reaction. After reaction, the reactor was cooled down to room temperature. The gas products were collected by a gas bag and analyzed by gas chromatograph (GC-900C, Shanghai) equipped with a 3 m TDX-01 stainless column and thermal conductivity detector. Liquid products were filtered to remove the solid catalyst powder and charged into a 10 ml glass vial and analyzed by a gas chromatograph (GC-900C, Shanghai) equipped with a flame ionization detector. A HP-INNO-WAX column (30 m \times 0.32 mm \times 0.25 μ m) was equipped to separate all components.

All products detected in the liquid were identified by a gas chromatography and mass spectrometry system (GC-MS, Agilent 6890) and quantified via an internal standard method and n-butanol was used as the internal standard. Conversion of glycerol was calculated as the mass ratio of the consumed glycerol in the reaction to the initial added glycerol. The selectivity was calculated based on the amount of products detected to be formed per the amount of glycerol actually reacted. For example, if one mole of glycerol was converted into one mole ethylene glycol and one mole of methane, the selectivity of ethylene glycol and methane was calculated as 66.7 and 33.3 %, respectively.

Results and discussion

Physicochemical properties

As summarized in Table 1, the specific surface areas, pore volumes and average pore diameters of Cu–Ni/ Al_2O_3 bimetallic catalysts were presented. The BET surface areas

of the 30Cu/ Al_2O_3 and 30Ni/ Al_2O_3 before reaction were 239.5 and 177.2 m^2/g , respectively. The introduction of Ni can remarkably increase the surface area of monometallic Cu/ Al_2O_3 sample even though the dosage of nickel accounted for as little as 5 wt%. At the same time, the pore volumes and pore diameters declined significantly because of Ni addition. This implied that Ni species effectively improved the dispersion of 30Cu/ Al_2O_3 . The promoted pores of Cu–Ni/ Al_2O_3 bimetallic catalysts were inclined to be smaller and more homogeneous. Moreover, the results also showed that the addition of ZnO to the 15Cu–15Ni/ Al_2O_3 catalyst changed the texture structure appreciably. The BET surface area and pore volume of 15Cu–15Ni/40ZnO– Al_2O_3 were 187.1 m^2/g and 0.37 cm^3/g , respectively. This was attributed to the ZnO material itself having low surface area and small pore volume, which resulted in blockage of part of the small pores. Compared with the used samples, all the surface areas and pore volumes decreased to varying degrees. This phenomenon might be due to the attrition of catalysts.

Figure 1 shows the XRD patterns of the Cu–Ni bimetallic catalysts reduced at 500 °C for 4 h. The diffraction peaks of γ - Al_2O_3 located at $2\theta = 37.6^\circ$, 45.9° and 67.0° were distinct even for catalysts with high content of Cu and Ni in the catalysts. The 30Cu/ γ - Al_2O_3 monometallic catalyst exhibited characteristic peaks for metallic Cu at $2\theta = 43.3^\circ$, 50.4° and 74.1° . The high intensity peak observed at the 2θ value of 43.3° was indexed to Cu(111). In the case of 30Ni/ γ - Al_2O_3 monometallic catalyst, diffraction peaks at $2\theta = 44.5^\circ$, 51.8° and 76.4° attributed to (111), (200) and (220) planes of Ni could be observed. As shown in Fig. 1 for all bimetallic samples, metallic phases of Cu, Ni and γ - Al_2O_3 were detected except for the differences of diffraction intensity. Gandarias et al. [21] believed that the formation

Table 1 Specific surface areas, pore volume and average pore diameter of fresh and spent samples

Catalysts	Fresh			Spent		
	S_{BET} ($m^2 \cdot g^{-1}$)	Pore volume ($cm^3 \cdot g^{-1}$)	Pore size (nm)	S_{BET} ($m^2 \cdot g^{-1}$)	Pore volume ($cm^3 \cdot g^{-1}$)	Pore size (nm)
30Ni/ Al_2O_3	239.5	0.39	6.4	210.2	0.33	6.3
25Ni–5Cu/ Al_2O_3	245.3	0.40	6.6	244.0	0.38	6.4
20Ni–10Cu/ Al_2O_3	242.7	0.40	6.0	239.5	0.37	5.8
15Ni–15Cu/ Al_2O_3	246.9	0.40	6.4	240.0	0.39	6.4
10Ni–20Cu/ Al_2O_3	239.1	0.40	6.6	233.9	0.37	6.4
5Ni–25Cu/ Al_2O_3	248.2	0.42	7.0	240.7	0.38	6.6
30Cu/ Al_2O_3	177.2	0.60	13.6	162.0	0.45	11.1
15Ni–15Cu/20ZnO– Al_2O_3	229.0	0.38	6.6	229.3	0.34	5.9
15Ni–15Cu/40ZnO– Al_2O_3	187.1	0.37	8.1	184.1	0.36	7.7
15Ni–15Cu/60ZnO– Al_2O_3	150.2	0.35	9.5	119.4	0.30	10.1
15Ni–15Cu/80ZnO– Al_2O_3	131.5	0.34	10.2	96.8	0.31	12.7
15Ni–15Cu/100ZnO– Al_2O_3	111.7	0.33	11.8	97.8	0.32	13.1

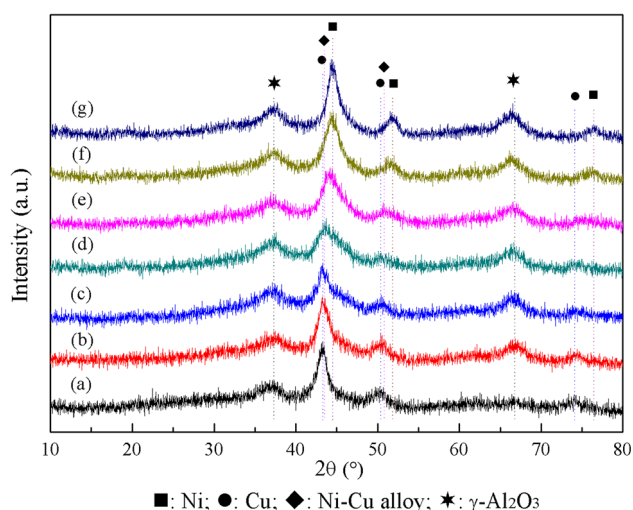


Fig. 1 XRD patterns of reduced Cu–Ni/Al₂O₃ catalysts. **a** 30Cu/Al₂O₃; **b** 25Cu–5Ni/Al₂O₃; **c** 20Cu–10Ni/Al₂O₃; **d** 15Cu–15Ni/Al₂O₃; **e** 10Cu–20Ni/Al₂O₃; **f** 5Cu–25Ni/Al₂O₃; **g** 30Ni/Al₂O₃

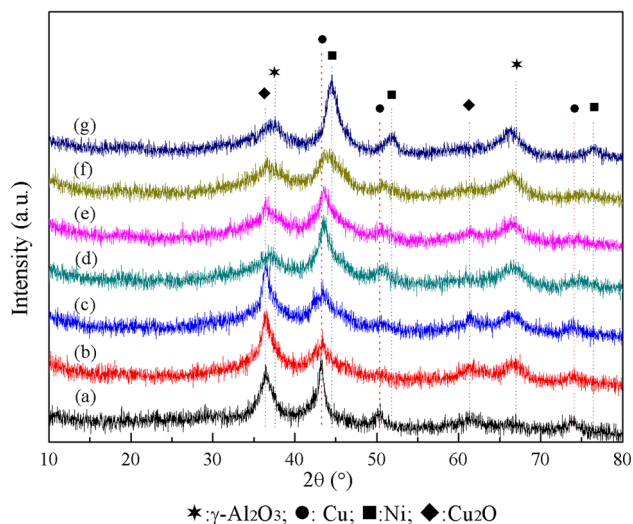


Fig. 2 XRD patterns of used Cu–Ni/Al₂O₃ catalysts. **a** 30Cu/Al₂O₃; **b** 25Cu–5Ni/Al₂O₃; **c** 20Cu–10Ni/Al₂O₃; **d** 15Cu–15Ni/Al₂O₃; **e** 10Cu–20Ni/Al₂O₃; **f** 5Cu–25Ni/Al₂O₃; **g** 30Ni/Al₂O₃

of the Ni–Cu alloy took place during the reduction, which was located at $2\theta = 43.5^\circ$ and 50.8° . It was the bimetallic synergic effect between copper and nickel that promoted its catalytic performance.

XRD patterns of the used Cu–Ni bimetallic catalysts are shown in Fig. 2. The diffraction peaks of 30Ni/γ-Al₂O₃ at $2\theta = 44.5^\circ$, 51.8° and 76.4° remained almost unchanged. However, the Cu₂O species emerged at $2\theta = 36.5^\circ$ and 61.3° for the used catalysts containing Cu component. This implied that the Cu metal species at 30Cu/γ-Al₂O₃ was oxidized into lower valence state of Cu⁺ species during reaction. With the increase of Ni content, the peaks of

Cu₂O disappeared gradually when the Cu/Ni mass ratio reached 15:15. On the one hand, it was proposed that the formation of Cu–Ni species (might be alloy) changed the electrical property of Cu atom so as to inhibit the oxidation of Cu. On the other hand, the phase transformation of species could result in catalyst deactivation, which would be solved effectively by Ni incorporation as indicated in the activity evaluation (shown in Table 2).

Figure 3 presents the patterns of 15Cu–15Ni/Al₂O₃ catalysts promoted by different ZnO amount from 0wt % to 100wt %. According to the results of XRD, diffraction peaks referring to ZnO were not detected but peaks of ZnAl₂O₄ phase appeared obviously at $2\theta = 31.2^\circ$, 36.8° , 44.8° , 55.7° , 59.3° , 65.2° and 77.3° . These peaks were also attributed to CuAl₂O₄ species. The absence of Cu and Ni peaks suggested that the metal particles were highly dispersed into the Al₂O₃ support so that it was beyond the detection limit of XRD [9]. Furthermore, ZnO introduction increased Lewis acidity of catalysts which was responsible for the synergistic effect between ZnO and 15Cu–15Ni/Al₂O₃ catalyst and enhanced the conversion of glycerol and selectivity of 1,2-PDO [22].

The reduction behavior of the Cu–Ni/Al₂O₃ catalysts was investigated by H₂-TPR and the results are shown in Fig. 4. The broad peak in the range of 600–800 °C corresponded to reduction of NiO species in intimate contact with Al₂O₃ support. The peak beyond 800 °C due to NiAl₂O₄ was not shown [23]. For the 30Cu/Al₂O₃ catalyst, the former peak in the range of 200–250 °C was attributed to highly dispersed CuO species and bulk CuO species started to be reduced at a temperature of around 270 °C [24]. However, the two reduction peaks were combined into one located at around 220 °C because of Ni introduction even though the amount was no more than 5wt %. With the increase of Ni content, the reduction peak shifted into higher temperature zone which was possibly attributed to the formation of Cu–Ni species. The XRD patterns also indicated the existence of Ni–Cu alloy.

Figure 5 shows H₂-TPR results of 15Ni–15Cu/Al₂O₃ catalysts promoted by different amount of ZnO. Without ZnO addition, the 15Ni–15Cu/Al₂O₃ catalyst exhibited only one reduction peak at 220 °C. As the ZnO loading increased, the peak moved downward to the lower temperature area and it was divided into two peaks until the ZnO content was more than 40wt %. This showed that ZnO could modify the interaction between metal oxides (CuO and NiO) and the support and favored the reduction of oxides. Besides, the introduction of ZnO enhanced the acidity on the catalyst surface, which was believed inclined to promote the dehydration of glycerol molecule and influence the reaction pathways.

Figure 6 shows the SEM images of fresh and spent catalysts. As can be seen, 15Ni–15Cu/Al₂O₃ catalyst

Table 2 Glycerol hydrogenolysis on Cu–Ni/Al₂O₃ bimetallic catalysts

Catalysts	Conversion/%	Selectivity/%				
		1,2-PDO	EG	Acetol	1-PO	Others ^a
30Ni/Al ₂ O ₃	77.0	68.6	13.2	4.1	5.0	9.1
5Cu–25Ni/Al ₂ O ₃	71.9	72.6	11.0	5.1	4.3	7.0
10Cu–20Ni/Al ₂ O ₃	73.0	75.5	8.7	5.9	4.1	5.8
15Cu–15Ni/Al ₂ O ₃	76.1	82.8	5.9	4.7	3.3	3.3
20Cu–10Ni/Al ₂ O ₃	72.6	75.6	5.1	14.4	2.1	2.8
25Cu–5Ni/Al ₂ O ₃	69.7	69.8	3.3	20.8	4.8	1.3
30Cu/Al ₂ O ₃	63.3	65.0	1.5	25.8	6.1	1.6

Reaction conditions: 1.0 g catalyst, 1.0 MPa N₂ pressure, 100 ml of 10wt % glycerol isopropanol solution, 8 h, 220 °C. *PDO* propanediol, *EG* ethylene glycol, *PO* propanol

^a Methane, CO₂, ethanol, 1,3-PDO, etc

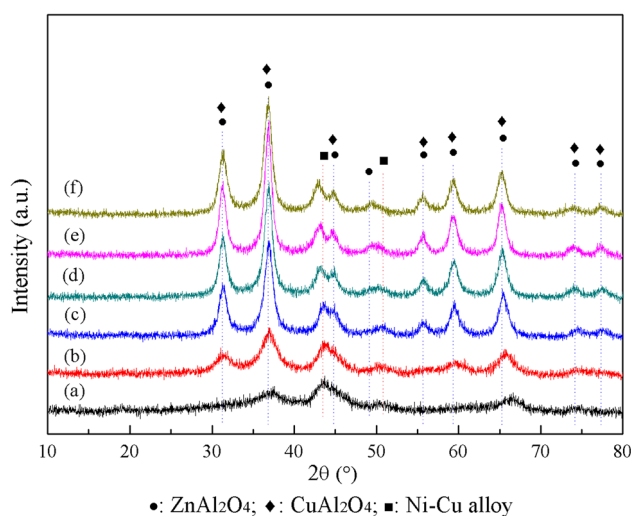


Fig. 3 XRD patterns of reduced Cu–Ni/ZnO–Al₂O₃ catalysts. **a** 15Cu–15Ni/Al₂O₃; **b** 15Cu–15Ni/20ZnO–Al₂O₃; **c** 15Cu–15Ni/40ZnO–Al₂O₃; **d** 15Cu–15Ni/60ZnO–Al₂O₃; **e** 15Cu–15Ni/80ZnO–Al₂O₃; **f** 15Cu–15Ni/100ZnO–Al₂O₃

suffered from sintering after use, and no visible carbon deposition and whisker were observed. The sintering would make the pore structure collapse and bring about low surface area as shown in Table 1. All these results maybe account for the decrease of catalyst activity. In contrast, the morphology of 15Ni–15Cu/40ZnO–Al₂O₃ catalyst remained stable by comparing the fresh and spent catalyst. And it also indicated that there was no carbon whisker formation.

Catalytic performance of Cu–Ni/Al₂O₃ bimetallic catalysts and ZnO-promoted catalysts

Conversion and selectivity data relative to the glycerol hydrogenolysis in the absence of added hydrogen over

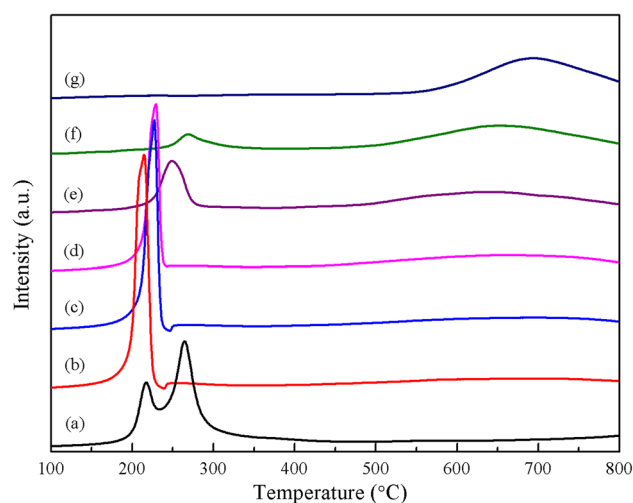


Fig. 4 H₂-TPR profiles of Cu–Ni/Al₂O₃ bimetallic catalysts. **a** 30Cu/Al₂O₃; **b** 25Cu–5Ni/Al₂O₃; **c** 20Cu–10Ni/Al₂O₃; **d** 15Cu–15Ni/Al₂O₃; **e** 10Cu–20Ni/Al₂O₃; **f** 5Cu–25Ni/Al₂O₃; **g** 30Ni/Al₂O₃

Cu–Ni/Al₂O₃ bimetallic catalysts with different Cu/Ni mass ratio are shown in Table 2. Among all the tested catalysts, the highest conversion was achieved over 30Ni/Al₂O₃ catalyst (77.0 %). In contrast, the 30Cu/Al₂O₃ catalyst exhibited the lowest activity for glycerol conversion (63.3 %). At the same time, the selectivity of intermediate acetol decreased along with the increase of Ni content. This implied that the Cu species favored the dehydration of glycerol molecule but the ability was deficient in hydrogenation of acetol compared with Ni species. However, Ni provided comparatively high activity in the C–C bond cleavage, so as to result in higher selectivity of C–C bond cleavage product such as EG and C1. In summary, the glycerol conversion and selectivity of 1,2-PDO over 15Cu–15Ni/Al₂O₃ reached 76.1 and 82.8 %, respectively, which was considered as the optimized catalyst.

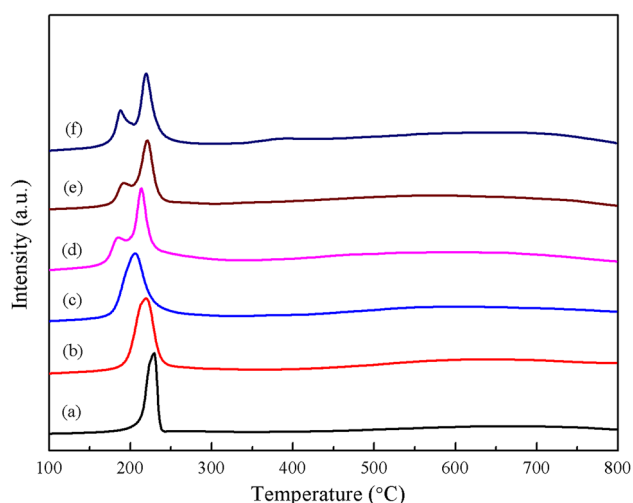


Fig. 5 H_2 -TPR profiles of Cu-Ni/ZnO- Al_2O_3 catalysts. **a** 15Cu-15Ni/ Al_2O_3 ; **b** 15Cu-15Ni/20ZnO- Al_2O_3 ; **c** 15Cu-15Ni/40ZnO- Al_2O_3 ; **d** 15Cu-15Ni/60ZnO- Al_2O_3 ; **e** 15Cu-15Ni/80ZnO- Al_2O_3 ; **f** 15Cu-15Ni/100ZnO- Al_2O_3

Fig. 6 SEM images of fresh and spent catalysts

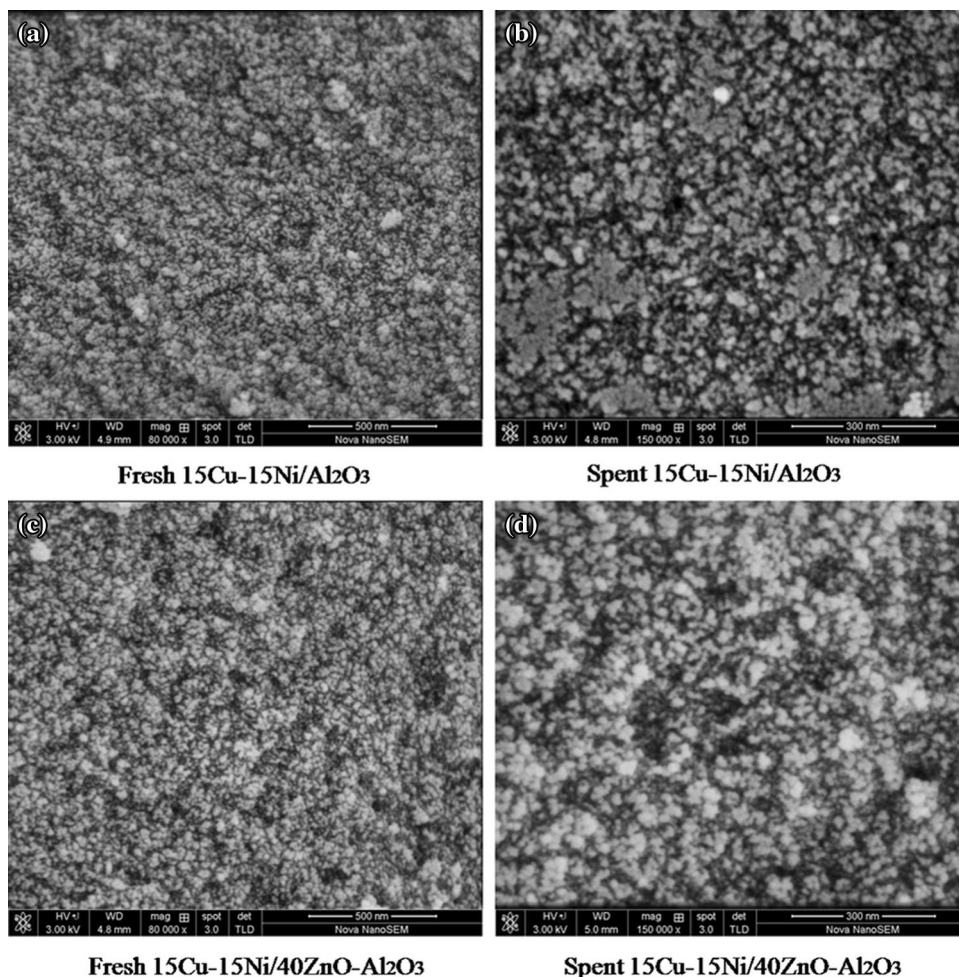


Table 3 presents the catalytic performance of 15Ni-15Cu/ Al_2O_3 catalysts modified by different ZnO dosage. When 40wt % of ZnO was added into 15Ni-15Cu/ Al_2O_3 catalyst, the glycerol conversion increased significantly from 76.1 to 82.0 %, with 86.7 % selectivity of 1,2-PDO. But as for higher concentration of ZnO-doped catalysts (60, 80 and 100 wt %), the catalysts exhibited declined activity. The lower activity may be attributed to coverage of active sites by ZnO and the blockage of pore structure. Moreover, the significant increase of selectivity of acetol was observed from all the ZnO-promoted catalysts. It was also reported by Hu that the introduction of ZnO to NiMo catalyst promoted the dehydration of glycerol to acetol and the hydrogenation of acetol to 1,2-PDO [28].

Figure 7 shows the time course of glycerol hydrogenolysis in the absence of added hydrogen over 15Ni-15Cu/40ZnO- Al_2O_3 catalyst at 220 °C and 1.0 MPa N_2 atmosphere. The conversion of glycerol increased quickly to 76.1 % in the first 8 h, and then increased smoothly to

Table 3 Glycerol hydrogenolysis on 15Cu–15Ni/Al₂O₃ catalysts promoted by ZnO

Catalysts	Conversion/%	Selectivity/%				
		1,2-PDO	EG	Acetol	1-PO	Others ^a
15Cu–15Ni/Al ₂ O ₃	76.1	82.8	5.9	4.7	3.3	3.3
15Cu–15Ni/20ZnO–Al ₂ O ₃	77.0	82.9	4.1	5.9	4.1	3.0
15Cu–15Ni/40ZnO–Al ₂ O ₃	82.0	86.7	3.3	6.6	1.6	1.8
15Cu–15Ni/60ZnO–Al ₂ O ₃	78.3	87.4	2.4	7.2	2.0	1.0
15Cu–15Ni/80ZnO–Al ₂ O ₃	69.4	84.5	1.9	9.4	2.9	1.3
15Cu–15Ni/100ZnO–Al ₂ O ₃	53.2	62.8	3.3	25.4	6.2	2.3

Reaction conditions: 1.0 g catalyst, 1.0 MPa N₂ pressure, 100 ml of 10wt % glycerol isopropanol solution, 8 h, 220 °C. *PDO* propanediol, *EG* ethylene glycol, *PO* propanol

^b Methane, CO₂, ethanol, 1,3-PDO, etc

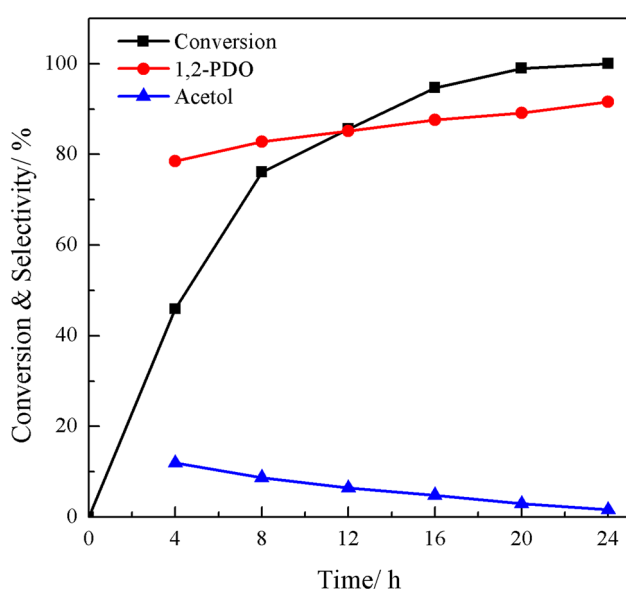


Fig. 7 Effect of reaction time on glycerol hydrogenolysis over 15Ni–15Cu/40ZnO–Al₂O₃ catalyst (Reaction conditions: 100 ml 10 %wt glycerol isopropanol solution, 1.0 g reduced catalyst, 220 °C, 1.0 MPa N₂)

100 % (20 h). It also can be seen that the selectivity of 1,2-PDO increased continuously from 78.5 to 91.6 % with increasing the reaction time. The selectivity of acetol decreased with the prolonged reaction time.

Recycling of the 15Ni–15Cu/40ZnO–Al₂O₃ catalyst was performed after washing with isopropanol in situ for several times. From Fig. 8, the used catalysts exhibited a slightly lower conversion. A gradual but minor decrease both in conversion and selectivity of 1,2-PDO could be observed, probably due to sintering, catalyst attrition and leaching of the active components. However, the glycerol conversion and 1,2-PDO selectivity of the fifth cycle still remained 73 and 79 %, respectively. In other words, the 15Ni–15Cu/40ZnO–Al₂O₃ catalyst showed a good potential for practical applicability.

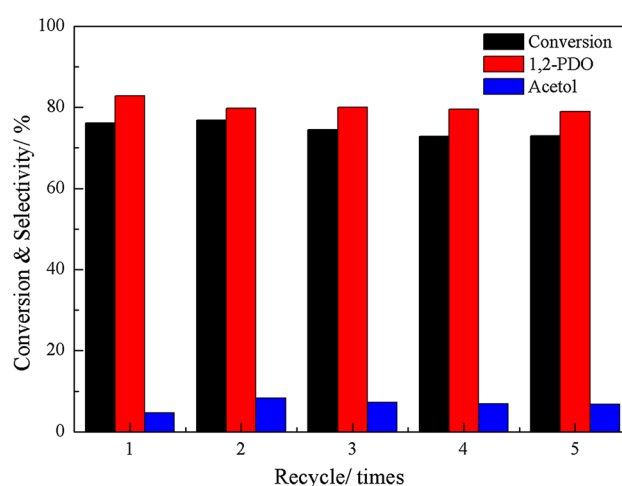


Fig. 8 Re-use of the 15Ni–15Cu/40ZnO–Al₂O₃ catalyst for glycerol hydrogenolysis. (Reaction conditions: 100 ml 10 %wt glycerol 2-propanol solution, 1.0 g reduced catalyst, 220 °C, 1.0 MPa N₂, 8 h)

In fact, there exists a competition of cleavage between the C–O and C–C bond. It is known that the selected support materials, types of metal and solvents greatly affect the reaction pathways and subsequent products distribution. Many reports proposed and confirmed that glycerol hydrogenolysis was conducted by “dehydration + hydrogenation” mechanism [25, 26]. Glycerol was first dehydrated to acetol over the acidic support and then acetol was hydrogenated into 1,2-PDO in the presence of metal catalyst.

When the CTH process was conducted under inert atmosphere, active hydrogen atoms formed from isopropanol can be transferred to an acceptor, or combined to produce H₂. As shown in Fig. 9, at first, the isopropanol was adsorbed on the Cu species and the O–H bond was dissociated to active hydrogen atoms. At the same time, isopropanol was converted into acetone which was detected by GC. Then, the oxygen on terminal OH groups of

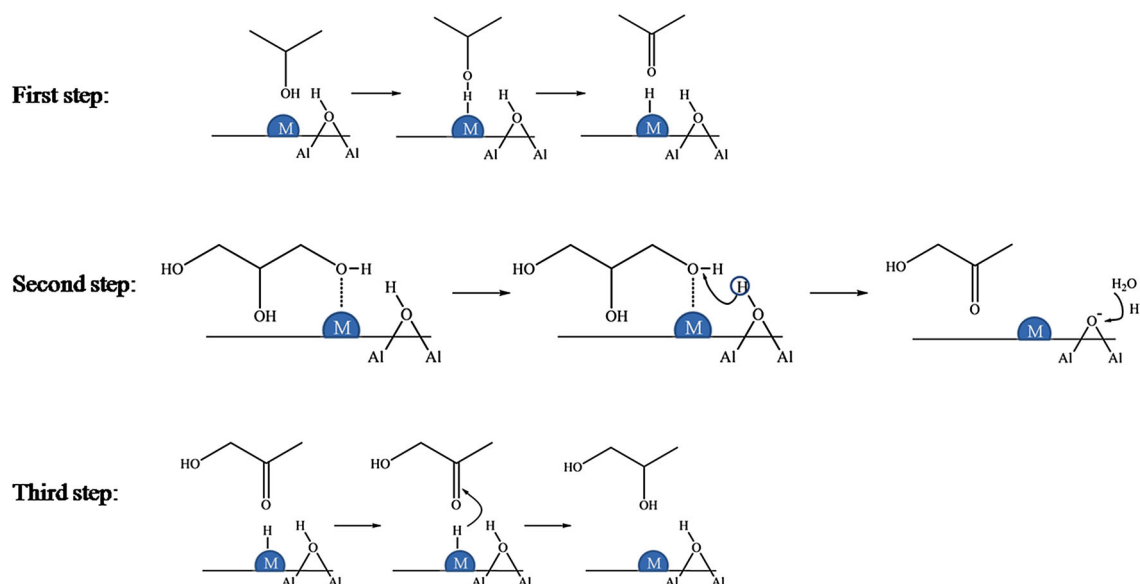


Fig. 9 Possible reaction pathways for glycerol hydrogenolysis using isopropanol as hydrogen donor molecule

glycerol was adsorbed on Cu metal, then the dehydration into acetol occurred at the acidic sites of the alumina support. In the absence of Ni, small amount of 1,2-PDO was produced because Cu possessed a weaker hydrogenation ability. The hydrides adsorbed on the metal attacked acetol molecule and converted it into 1,2-PDO. In general, Ni is active in the hydrogenolysis of glycerol both for C–C and C–O bonds cleavage to a similar extent. When Cu was introduced into the catalysts together with Ni, the selectivity to EG significantly decreased (see Table 2). Above XRD results confirmed the formation of Ni–Cu alloy in the bimetallic Cu–Ni/Al₂O₃ catalyst. It was also proved by Gandarias et al. [27, 28] that the formation of a Ni–Cu alloy reduces Ni ensemble size and the C–C hydrogenolysis activity. It was also reported that the incorporation of ZnO improved the dispersion of metal particles and reduced the particle size, which provided more active metal sites for the acetol hydrogenation. Moreover, the presence of ZnO supplied more acid sites for the dehydration of glycerol and prevented the sintering of catalyst.

Conclusion

The experimental results indicated that Cu–Ni/Al₂O₃ bimetallic catalysts prepared by coprecipitation method were suitable catalysts for glycerol conversion into 1,2-PDO in the absence of added hydrogen. The optimized mass ratio of Cu/Ni was 15:15, and the addition of ZnO into 15Cu–15Ni/Al₂O₃ could improve its catalytic performance and suppress the formation of C–C cleavage product. The best performance of 15Cu–15Ni/40ZnO–Al₂O₃

catalyst exhibited the glycerol conversion of 82.0 % and 1,2-PDO selectivity of 86.7 %, respectively. XRD revealed that the introduction of Ni into Cu monometallic catalyst suppressed the oxidation of Cu into Cu₂O species and promoted the formation of Ni–Cu alloy. H₂-TPR suggested that the addition of ZnO decreased the reduction temperature of Cu–Ni/Al₂O₃ catalyst and was beneficial to improvement of 1,2-PDO selectivity due to the enhanced surface acidity. In the end, ZnO doping was demonstrated to prevent the sintering phenomenon and thus enhanced its activity over 15Cu–15Ni/Al₂O₃.

Acknowledgments This work was supported by the National Natural Science Foundation of China (21373083) and the Open Project of State Key Laboratory of Chemical Engineering (SKL-ChE-12C03).

Open Access This article is distributed under the terms of the Creative Commons Attribution 4.0 International License (<http://creativecommons.org/licenses/by/4.0/>), which permits unrestricted use, distribution, and reproduction in any medium, provided you give appropriate credit to the original author(s) and the source, provide a link to the Creative Commons license, and indicate if changes were made.

References

1. Huber GW, Corma A (2007) Synergies between Bio- and Oil Refineries for the Production of Fuels from Biomass. *Angew Chem Int Ed* 46:7184–7201
2. Christensen CH, Rass-Hansen J, Marsden CC, Taarning E, Egeblad K (2008) The renewable chemicals industry. *ChemSusChem* 1(4):283–289
3. Besson M, Gallezot P, Pinel C (2013) Conversion of biomass into chemicals over metal catalysts. *Chem Rev* 114:1827–1870

4. Atabani AE, Silitonga AS, Badruddin IA, Mahlia TMI, Masjuki HH, Mekhilef S (2012) A comprehensive review on biodiesel as an alternative energy resource and its characteristics. *Renew Sustain Energy Rev* 16:2070–2093
5. Zhou CH, Zhao H, Tong DS, Wu LM, Yu WH (2013) Recent advances in catalytic conversion of glycerol. *Catal Rev* 55:369–453
6. Martin A, Armbruster U, Gandarias I, Arias PL (2013) Glycerol hydrogenolysis into propanediols using in situ generated hydrogen—a critical review. *Eur J Lipid Sci Technol* 115:9–27
7. Feng J, Xiong W, Xu B, Jiang W, Wang J, Chen H (2014) Basic oxide-supported Ru catalysts for liquid phase glycerol hydrogenolysis in an additive-free system. *Catal Commun* 46:98–102
8. Deng C, Duan X, Zhou J, Chen D, Zhou X, Yuan W (2014) Size effects of Pt-Re bimetallic catalysts for glycerol hydrogenolysis. *Catal Today* 234:208–214
9. Jiang T, Huai Q, Geng T, Ying W, Xiao T, Cao F (2015) Catalytic performance of Pd-Ni bimetallic catalyst for glycerol hydrogenolysis. *Biomass Bioenergy* 78:71–79
10. Koso S, Watanabe H, Okumura K, Nakagawa Y, Tomishige K (2012) Comparative study of Rh–MoO_x and Rh–ReO_x supported on SiO₂ for the hydrogenolysis of ethers and polyols. *Appl Catal B Environ* 111–112:27–37
11. Yu W, Zhao J, Ma H, Miao H, Song Q, Xu J (2010) Aqueous hydrogenolysis of glycerol over Ni–Ce/AC catalyst: promoting effect of Ce on catalytic performance. *Appl Catal A Gen* 383:73–78
12. Balaraju M, Jagadeeswarai K, Prasad PSS, Lingaiah N (2012) Catalytic hydrogenolysis of biodiesel derived glycerol to 1,2-propanediol over Cu–MgO catalysts. *Catal Sci Technol* 2:1967–1976
13. Guo X, Li Y, Shi R, Liu Q, Zhan E, Shen W (2009) Co/MgO catalysts for hydrogenolysis of glycerol to 1, 2-propanediol. *Appl Catal A Gen* 371:108–113
14. D'Hondt E, Van de Vyver S, Sels BF, Jacobs PA (2008) Catalytic glycerol conversion into 1,2-propanediol in absence of added hydrogen. *Chem Commun* 45:6011–6012
15. Wawrzetz A, Peng B, Hrabar A, Jentys A, Lemonidou AA, Lercher JA (2010) Towards understanding the bifunctional hydrodeoxygenation and aqueous phase reforming of glycerol. *J Catal* 269:411–420
16. Gandarias I, Arias PL, Fernández SG, Requies J, El Doukkali M, Güemez MB (2012) Hydrogenolysis through catalytic transfer hydrogenation: glycerol conversion to 1,2-propanediol. *Catal Today* 195:22–31
17. Gandarias I, Arias PL, Requies J, El Doukkali M, Güemez MB (2011) Liquid-phase glycerol hydrogenolysis to 1,2-propanediol under nitrogen pressure using 2-propanol as hydrogen source. *J Catal* 282:237–247
18. Musolino MG, Scarpino LA, Mauriello F, Pietropaolo R (2009) Selective transfer hydrogenolysis of glycerol promoted by palladium catalysts in absence of hydrogen. *Green Chem* 11:1511–1513
19. Gandarias I, Fernández S, El Doukkali M, Requies J, Arias P (2013) Physicochemical study of glycerol hydrogenolysis over a Ni–Cu/Al₂O₃ catalyst using formic acid as the hydrogen source. *Top Catal* 56:995–1007
20. Xia S, Zheng L, Wang L, Chen P, Hou Z (2013) Hydrogen-free synthesis of 1,2-propanediol from glycerol over Cu–Mg–Al catalysts. *RSC Adv* 3:16569–16576
21. Gandarias I, Requies J, Arias PL, Armbruster U, Martin A (2012) Liquid-phase glycerol hydrogenolysis by formic acid over Ni–Cu/Al₂O₃ catalysts. *J Catal* 290:79–89
22. Panyad S, Jongpatiwut S, Sreethawong T, Rirksomboon T, Osuwan S (2011) Catalytic dehydroxylation of glycerol to propylene glycol over Cu–ZnO/Al₂O₃ catalysts: effects of catalyst preparation and deactivation. *Catal Today* 174:59–64
23. Cai X, Dong X, Lin W (2008) Effect of CeO₂ on the catalytic performance of Ni/Al₂O₃ for autothermal reforming of methane. *J Nat Gas Chem* 17:98–102
24. López-Suárez FE, Bueno-López A, Illán-Gómez MJ (2008) Cu/Al₂O₃ catalysts for soot oxidation: copper loading effect. *Appl Catal B Environ* 84:651–658
25. Dasari MA, Kiatsimkul P-P, Sutterlin WR, Suppes GJ (2005) Low-pressure hydrogenolysis of glycerol to propylene glycol. *Appl Catal A Gen* 281(1–2):225–231
26. Miyazawa T, Kusunoki Y, Kunimori K, Tomishige K (2006) Glycerol conversion in the aqueous solution under hydrogen over Ru/C + an ion-exchange resin and its reaction mechanism. *J Catal* 240:213–221
27. Hu J, Liu X, Wang B, Pei Y, Qiao M, Fan K (2012) Reforming and hydrogenolysis of glycerol over Ni/ZnO catalysts prepared by different methods. *Chin J Catal* 33:1266–1275
28. Hu J, Liu X, Fan Y, Xie S, Pei Y, Qiao M, Fan K, Zhang X, Zong B (2013) Physically mixed ZnO and skeletal NiMo for one-pot reforming-hydrogenolysis of glycerol to 1,2-propanediol. *Chin J Catal* 34:1020–1026